



Cite this: DOI: 10.1039/d3dt03741j

Received 9th November 2023,
Accepted 19th December 2023

DOI: 10.1039/d3dt03741j

rsc.li/dalton

Open-cage fullerenes as ligands for metals

Alan L. Balch 

The remarkable structures of open-cage fullerenes with functionalization on the outer surface and an accessible inner void make them interesting ligands for reactions with metal complexes. The behaviors of open-cage fullerenes in reactions with various metal complexes are examined and compared to the corresponding reactions with intact fullerenes. The structural results from X-ray diffraction are emphasized. Open-cage fullerenes frequently undergo unanticipated structural changes such as carbon–carbon bond cleavage upon reactions with metal complexes. Much more remains to be learned about the possibility of inserting metal ions larger than Li^+ into the interior void of these open-cage fullerenes and about the effects of redox reactions on metal complexes of open-cage fullerenes.

Introduction

After the discovery that C_{60} could be obtained in macroscopic amounts,¹ chemists seized on the opportunity to chemically modify the readily accessible outer surface of this highly symmetrical molecule.² One approach involved the creation of openings in the fullerene cage that could allow small molecules and atoms to enter the interior void to produce endohedral fullerenes.^{3,4} Eventually, a wide array of open-cage fullerenes were prepared, and their abilities to host guest molecules in their interior were explored.^{5–7} The use of the “molecular surgery” approach allowed endohedral fullerenes such as $\text{H}_2@\text{C}_{60}$ and $\text{H}_2\text{O}@\text{C}_{60}$ to be synthesized by chemically preparing an open-cage fullerene, inserting the small molecule and then chemically closing the opening.^{8,9} Other species that have been introduced into the interior of open-cage fullerenes include NH_3 , H_2O_2 , CH_4 , and rare gasses.⁷

Fig. 1 shows drawings of a representative example of an open-cage fullerene, **MMK-15**, as determined by single crystal X-ray diffraction¹⁰ (we used the authors' initials followed by the number used in the original article to designate this and other open-cage molecules discussed here). The picture on the left shows a conventional thermal ellipsoid drawing of the molecule with the carbons atoms of the 13-membered orifice colored dark blue and the two keto groups with the red oxygen atoms on opposite sides of the rim. An imine nitrogen atom and a sulfur atom are part of the cage opening. The picture on the right shows a space-filling drawing of the same molecule from a perspective that looks through the opening into the cage. The sliver of grey at the center between the two red

oxygen atoms is the orifice that allows us to see the opposite side of the cage interior. While small, this opening is large enough to allow dihydrogen to enter the fullerene cavity to produce the endohedral $\text{H}_2@\text{MMK-15}$.⁹

In addition to hosting rare gasses and small molecules, endohedral fullerenes can contain one to four metal atoms, sometimes along with main group atoms that form clusters.^{11–13} In general, endohedral metallofullerenes are obtained in low yields by a gas phase process that involves electric arc vaporization of graphite rods doped with an appropriate metal oxide. However, until very recently, metal ions have not been found to enter the interior of open-cage fullerenes (*vide infra*). Nevertheless, the ability to insert metal atoms or ions into open-cage fullerenes could provide a means to obtain such guest/host molecules in higher yields compared to the current gas phase processes. If endohedral metallofullerenes became available in greater quantities, then some of their potential uses (gadolinium endohedral complexes as magnetic resonance imaging (MRI) relaxation agents,^{14–16} lutetium endohedral complexes as X-ray contrast agents and radiodiagnostic agents,^{17,18} etc.) might be realized.

In this perspective, the use of open-cage fullerenes as ligands will be reviewed. There are several properties of open-cage fullerenes that make them interesting ligands. The cage architecture itself provides an unusual and attractive framework for coordination. Moreover, open-cage fullerenes retain some of the electrochemical behavior that is observed with intact fullerenes and can be used to introduce redox functionality into their metal complexes.^{19–21} Additionally, open-cage fullerenes are chromophores with absorption extending in the visible and near IR regions. Cage-opening reactions can also add Lewis basic functional groups around the orifice that may be used to bind metal centers. This article will examine the coordination of metal centers to open-cage fullerenes and will compare the bonding of the same metal centers to C_{60} . The

Department of Chemistry, University of California, One Shields Avenue, Davis, CA, USA. E-mail: albalch@ucdavis.edu; Fax: +1 (530) 752 2820; Tel: +1 (530) 752 0941

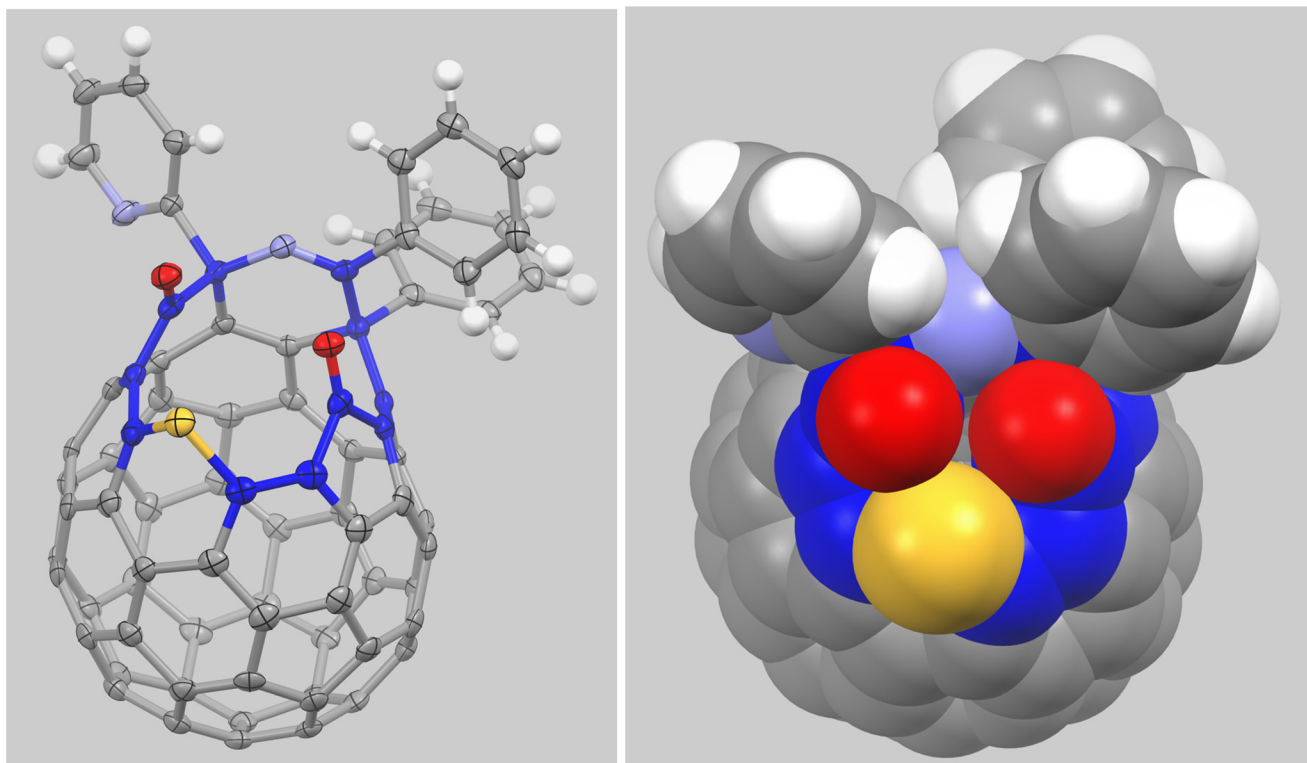


Fig. 1 Drawings of a representative open-cage fullerene, **MMK-15**. Left, a drawing using thermal ellipsoids. Right, a space-filling drawing from a perspective that looks down on the opening into the cage. Color scheme: carbon, grey except for those on the rim of the opening which are dark blue; hydrogen, white; nitrogen, pale blue; oxygen, red; sulfur, yellow. From data in Y. Murata, M. Murata and K. Komatsu, *Chem. Eur. J.*, 2003, **9**, 1600–9.

coordination of metal complexes to pristine C_{60} and other fullerenes has been reviewed.^{22,23} In general, η^2 -bonding to the 6:6 ring junctions of C_{60} is the dominant means of attachment of single metal centers to C_{60} ,^{24,25} although cases of η^1 -bonding are known.²⁶ Metal clusters are also known to bind to C_{60} in a variety of fashions.²⁷ A related topic, the behavior of functionalized, but intact, fullerenes as ligands, has also been reviewed.²⁸

A major focus of this article concerns the structures of complexes of open-cage fullerenes with metal centers as determined by single crystal X-ray diffraction, since this technique offers the best means to understand the three dimensional nature of these complex molecules. A nice review of a related topic, the coordination of metal complexes to buckybowls, polycyclic hydrocarbon molecules that map onto the surface of C_{60} such as corannulene, is available,²⁹ as is a review on metal ion coordination to reduced buckybowls and related hydrocarbon anions.³⁰ In general, these buckybowls have a modest curvature that produces an interior that is considerably more open than the interior cavities of open-cage fullerenes discussed here.

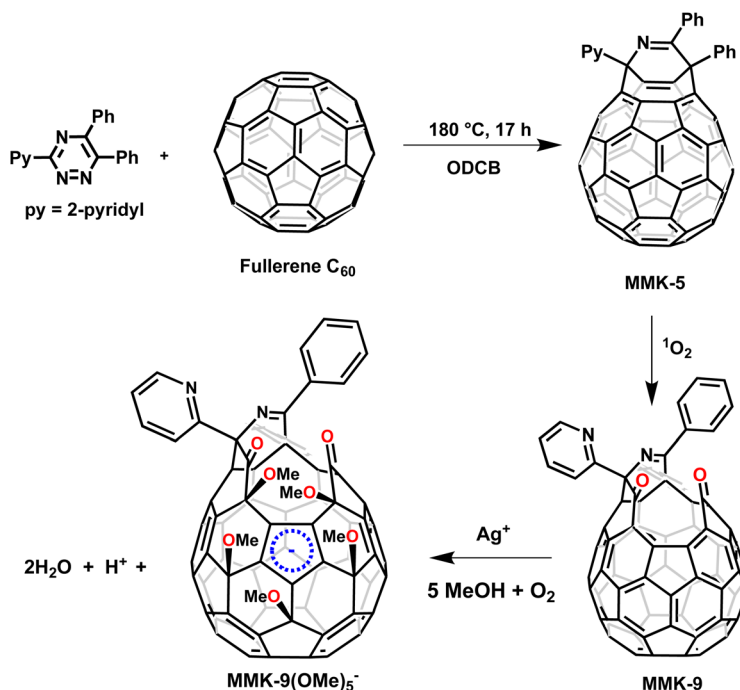
The unexpected reactivity of the open-cage fullerene **MMK-9**

The open-cage fullerene **MMK-9** is readily available from C_{60} by a two-step synthetic route shown in Scheme 1.¹⁰ The struc-

ture of **MMK-9** as determined by single crystal X-ray diffraction is shown in Fig. 2. **MMK-9** possesses a 12-membered-ring orifice which is highlighted in blue in Fig. 2. The opening in this cage appears to be too small to allow small molecules to enter the interior of the molecule.³¹

Reactions with silver(I) salts

Allowing a methanol solution of silver trifluoroacetate to diffuse into a dichloromethane solution of **MMK-9** open to the atmosphere produced black crystals of $\{\text{MMK-9}(\text{OCH}_3)_5\text{Ag}(\text{AgO}_2\text{CCF}_3)\}_2 \cdot 4\text{CH}_2\text{Cl}_2$.³² There are several interesting features of this compound. Remarkably, five CH_3O groups have been added to the open-cage fullerene at the ends of the five double bonds that radiate from a pentagon just below the cage opening (shown in Fig. 3) to yield a mono-anionic open-cage fullerene. This pattern of addition of OMe groups is similar to the addition pattern of phenyl or methyl groups observed in the preparation of $(\eta^5\text{-}C_{60}\text{Ph}_5)\text{Tl}$ and the ferrocene/[C_{60}]fullerene hybrid $(\eta^5\text{-}C_{60}\text{Me}_5)\text{Fe}(\eta^5\text{-}C_5\text{H}_5)$ both of which begin with the reaction of Me_2SCuBr and RMgBr ($\text{R} = \text{Ph}$ or Me) with C_{60} .^{33,34} In contrast to the air-sensitive syntheses like those just mentioned, the reaction that produces $\{\text{MMK-9}(\text{OCH}_3)_5\text{Ag}(\text{AgO}_2\text{CCF}_3)\}_2 \cdot 4\text{CH}_2\text{Cl}_2$ requires exposure to air. It appears that dioxygen is the oxidant that added the five CH_3O groups to the open-cage fullerene. If the reaction is conducted under an inert atmosphere, no crystals form. There is no evidence that



Scheme 1 Formation of MMK-9 and its reaction with methanol in the presence of Ag^+ and dioxygen.

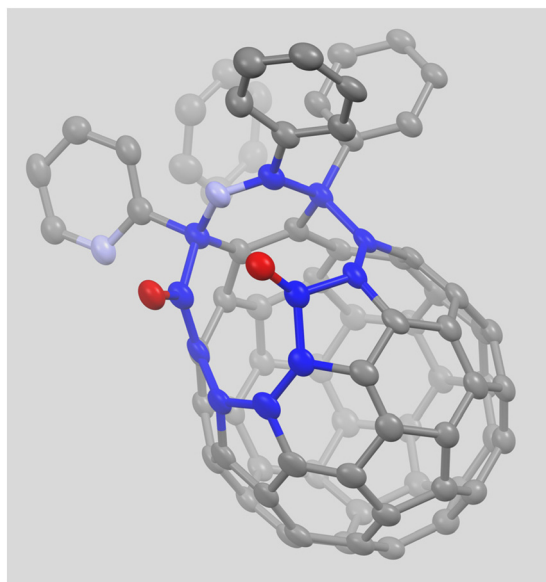


Fig. 2 The structure of the open-cage fullerene **MMK-9**. Color scheme: carbon, grey except for those on the rim of the opening which are dark blue; nitrogen, pale blue; oxygen, red. From data in A. Aghabali, S. Jun, M. M. Olmstead, and A. L. Balch, *J. Am. Chem. Soc.*, 2016, **138**, 16459–65.

silver is reduced in the process. The addition of five CH_3O groups is a unique reaction that occurs with **MMK-9**. Under comparable conditions, C_{60} does not react in this fashion. However, in ethanol solution in air, silver(I) nitrate

does react with C_{60} to produce black crystals of $\text{C}_{60}\{\text{Ag}(\text{NO}_3)\}_5$ in which a network of silver nitrate ions surrounds each fullerene.³⁵

The bonding of silver ions to the open cages is another interesting feature of this molecule. There are two silver ions in the asymmetric unit. One is at the periphery of the molecule and chelated by the two nitrogen atoms of the trifluoroacetate ion and by an oxygen atom of the trifluoroacetate ion. The other silver ion (Ag1) is coordinated by two methoxy groups and is η^2 -coordinated to two carbon atoms at a 5:6 ring junction on the open-cage fullerene. In the centrosymmetric dimer, Ag1 is also bonded to its symmetry generated counterpart Ag1' with an Ag1–Ag1' distance of 2.8368(12) Å. Such a short Ag1–Ag1' distance indicates that there is an argentophilic interaction at the center of the dimer.³⁶ Additionally, each of the two central silver ions forms an η^1 bond to a fullerene cage in the adjoining open cage. Thus, each of the central silver ions interacts with the adjacent silver ion, four methoxy groups (two from each open cage), two carbon atoms from one open cage and one carbon atom on the other open cage.

Black crystals containing polymeric $[\{\text{MMK-9(OCH}_3)_5\text{Ag}(\text{AgOCH}_3)\}_2\text{H}_2\text{O}]$, are formed when a dichloromethane solution of **MMK-9** was slowly diffused to a methanol solution of silver nitrate again with exposure to air. These crystals contain the same modification of **MMK-9** in which five CH_3O units are added to each open-cage fullerene and similar dimerization of two open cages about a pair of closely connected silver ions (Ag–Ag distances: 2.853(1) and 2.863(1) Å) as shown in Fig. 3. To complicate matters, there are two open-cage fullerenes in the

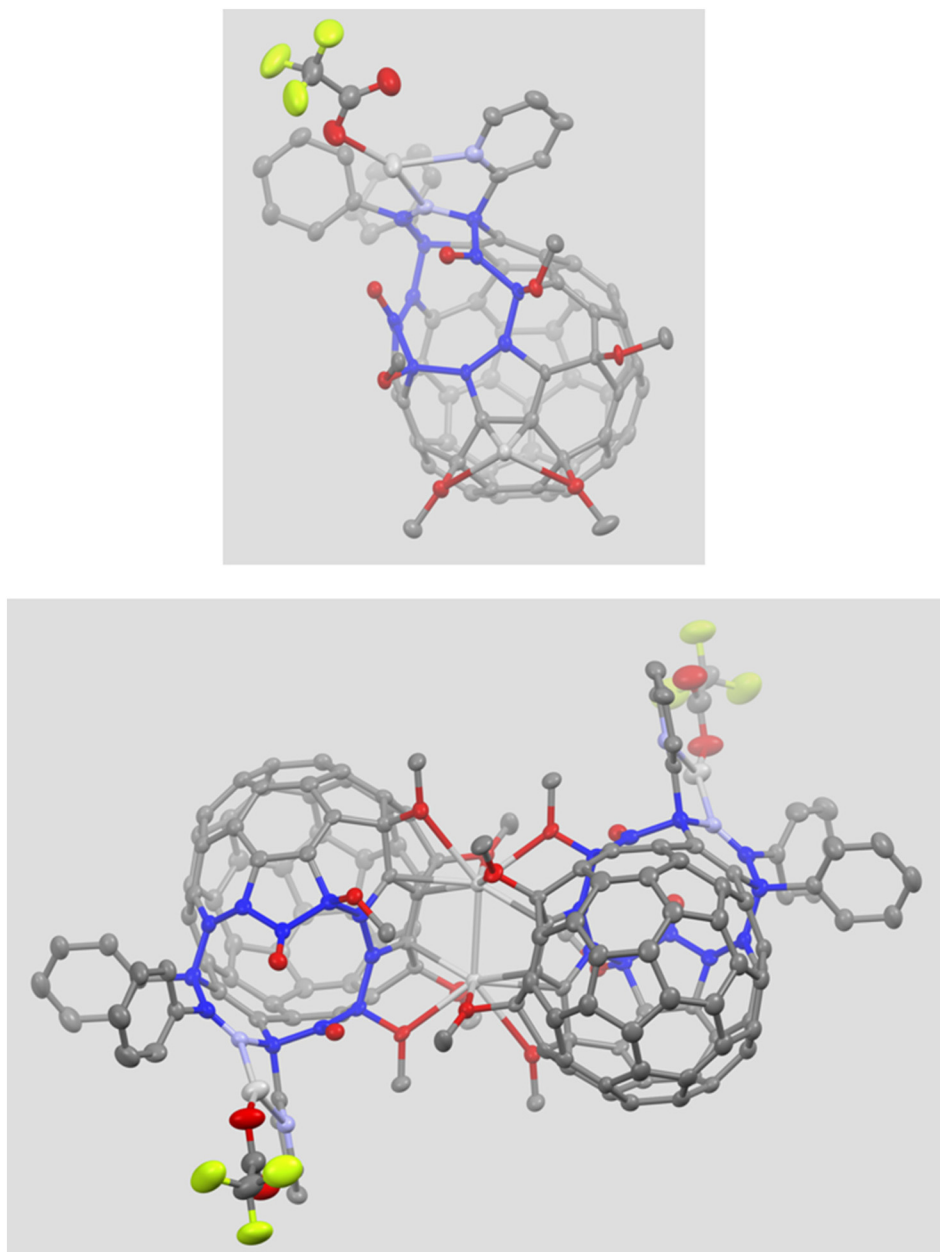


Fig. 3 The structure of $\{\text{MMK-9-(OCH}_3)_5\text{Ag(AgO}_2\text{CCF}_3\text{)}\}_2$ with hydrogen atoms removed for clarity. Top, the asymmetric unit. Bottom, the complete centrosymmetric dimer. Color scheme: carbon, grey except for those atoms on the rim of the opening which are dark blue; nitrogen, pale blue; oxygen, red; silver, white; fluorine, yellow. From data in A. Aghabali, S. Jun, M. M. Olmstead and A. L. Balch, *J. Am. Chem. Soc.*, 2016, **138**, 16459–65.

asymmetric unit, but both have similar structures and both pack about centers of symmetry. Polymerization occurs due to coordination of a silver ion that is chelated by the two nitrogen atoms of one open cage to a pair of carbon atoms at a 6 : 6 ring junction on the periphery of an adjacent open cage. This arrangement can be seen at the top and bottom of Fig. 4. Charge balance is achieved by the presence of a loosely bound methoxide ion that is near the silver ions chelated by two nitrogen atoms. Neither $\{\text{MMK-9(OCH}_3)_5\text{Ag(AgO}_2\text{CCF}_3\text{)}\}_2\cdot 4\text{CH}_2\text{Cl}_2$

nor $[\{\text{MMK-9(OCH}_3)_5\text{Ag(AgOCH}_3\text{)}\}_2\cdot \text{H}_2\text{O}]_n$ is soluble in organic solvents or water. Consequently, the solution properties of these compounds could not be studied.

Reaction with $(\text{Ph}_3\text{P})_4\text{Pt}$

Addition of $(\text{Ph}_3\text{P})_4\text{Pt}$ to **MMK-9** in dioxygen-free toluene produced the adduct $(\text{Ph}_3\text{P})_2\text{Pt-}\text{MMK-9}$ in 46% yield after 90 minutes of stirring at room temperature.³⁷ The structure of the adduct is shown in Fig. 5. Remarkably, a platinum

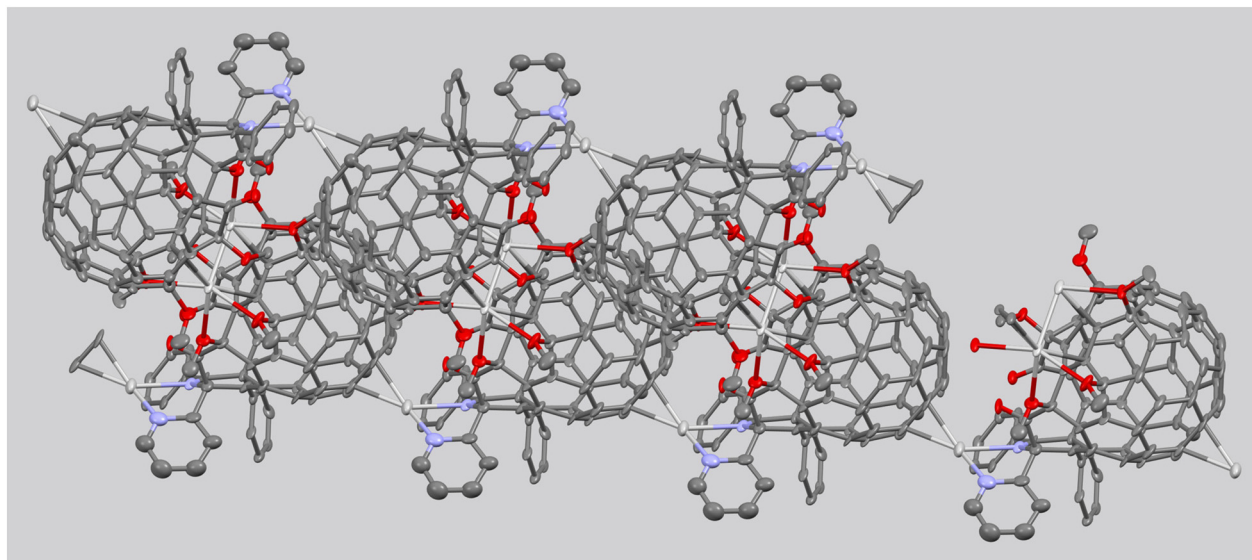


Fig. 4 The structure of one of the two polymeric chains in $\{[\text{MMK-9}(\text{OCH}_3)_5\text{Ag}(\text{AgOCH}_3)_2\cdot\text{H}_2\text{O}\}_n$. Color scheme: carbon, grey; nitrogen, pale blue; oxygen, red; silver, white. Hydrogen atoms, the loosely bound methoxide ions near the silver ions chelated by two nitrogen atoms, and the solvate water molecules were omitted for clarity. From data in A. Aghabali, S. Jun, M. M. Olmstead and A. L. Balch, *J. Am. Chem. Soc.*, 2016, **138**, 16459–65.

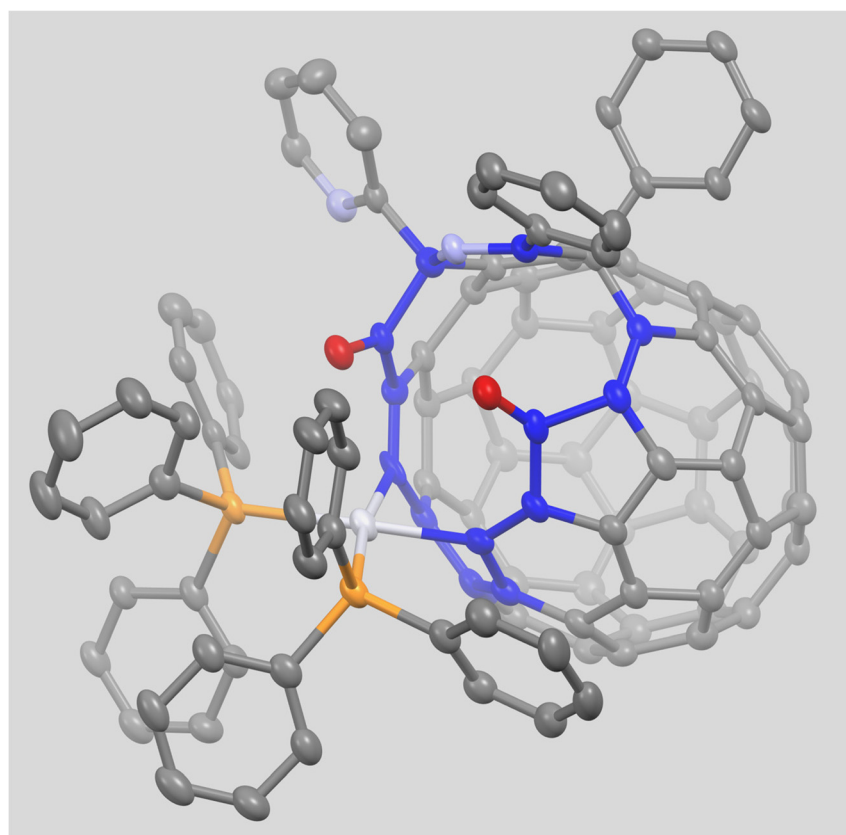


Fig. 5 The structure of $(\text{Ph}_3\text{P})_2\text{Pt-MMK-9}$. Color scheme: carbon, grey except for those on the rim of the opening which are dark blue; nitrogen, pale blue; oxygen, red; platinum white; phosphorus, orange. From data in S. R. Gralinski, M. Roy, L. M. Baldauf, M. M. Olmstead and A. L. Balch, *Chem. Commun.*, 2016, **138**, 16459–65.

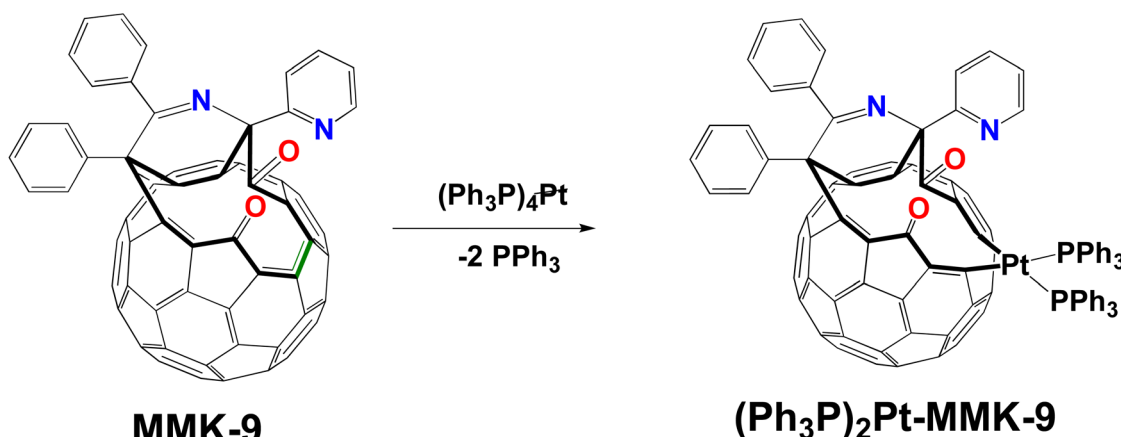
atom inserted itself into a C–C bond of the open-cage fullerene to become part of the fabric of the fullerene cage. In $(\text{Ph}_3\text{P})_2\text{Pt-MMK-9}$, the distance between the two carbon atoms coordinated to platinum is 2.59(1) Å, whereas the corresponding C–C bond length in **MMK-9** is 1.533(5) Å. For comparison, in $(\text{Ph}_3\text{P})_2\text{Pt}(\eta^2\text{-C}_60)$, the Pt–C bond lengths are 2.145(24) and 2.115(23) and the C–C bond length is 1.502(30) Å.²²

$(\text{Ph}_3\text{P})_2\text{Pt-MMK-9}$ is soluble in toluene, carbon disulfide, and *o*-dichlorobenzene. It is quite stable at room temperature and survives chromatography on silica gel. Cyclic voltammetry in *o*-dichlorobenzene reveals that $(\text{Ph}_3\text{P})_2\text{Pt-MMK-9}$ undergoes a one-electron reduction at a potential considerably more negative than that of **MMK-9** itself.³⁷

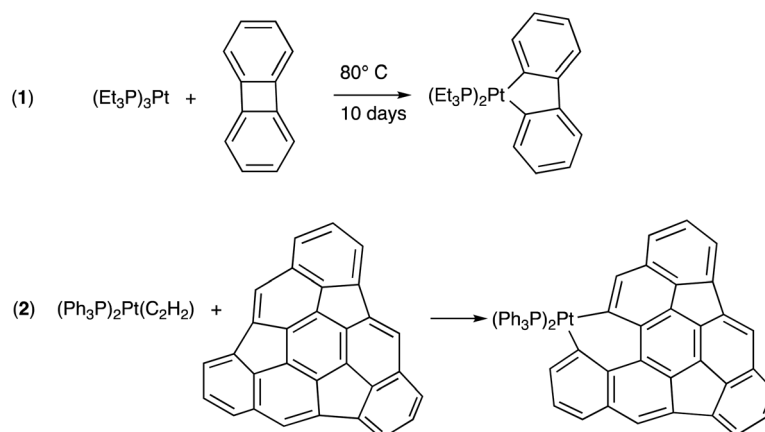
Two other related oxidative addition reactions involving C–C bond breaking and oxidative addition to Pt(0) are outlined in Scheme 2. Both require higher temperatures and longer

reaction times than needed for the addition of $(\text{Ph}_3\text{P})_4\text{Pt}$ to **MMK-9**. As shown in reaction (1) in Scheme 3, biphenylene reacts with $(\text{Et}_3\text{P})_3\text{Pt}$ at 80 °C for 10 days to produce the C–C bond cleavage product.³⁸ As shown in reaction (2) in Scheme 3, the semi-buckminsterfullerene ($\text{C}_{30}\text{H}_{12}$) requires 15 h of reaction in toluene followed by one hour of heating under reflux with $(\text{Ph}_3\text{P})_2\text{Pt}(\text{C}_2\text{H}_4)$ to produce only 5–10% yield of the C–C bond cleavage product.³⁹

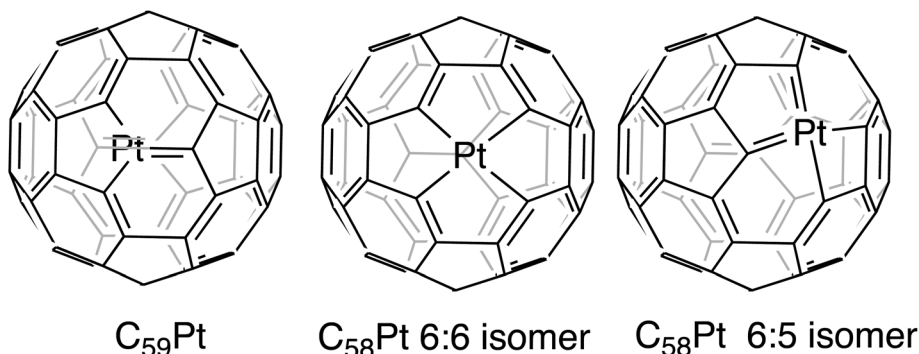
The formation of $(\text{Ph}_3\text{P})_2\text{Pt-MMK-9}$ offers a suggestion that heterofullerenes containing platinum may be eventually synthesized through a solution chemical means, since $(\text{Ph}_3\text{P})_2\text{Pt-MMK-9}$ has a platinum atom as an integral part of the cage itself. The heterofullerenes C_{59}Pt and C_{58}Pt shown in Scheme 4, in which a platinum atom replaces one or two carbon atoms in C_{60} , have been detected in mass spectrometric studies of the laser ablation of the electrochemically deposited films of C_{60} and platinum.^{40,41} Their



Scheme 2 The reaction of **MMK-9** with $(\text{Ph}_3\text{P})_4\text{Pt}$.



Scheme 3 Examples of carbon–carbon bond cleavage by the oxidative addition of $(\text{R}_3\text{P})_2\text{Pt}^0$.



Scheme 4 Platinum-containing heterofullerenes.

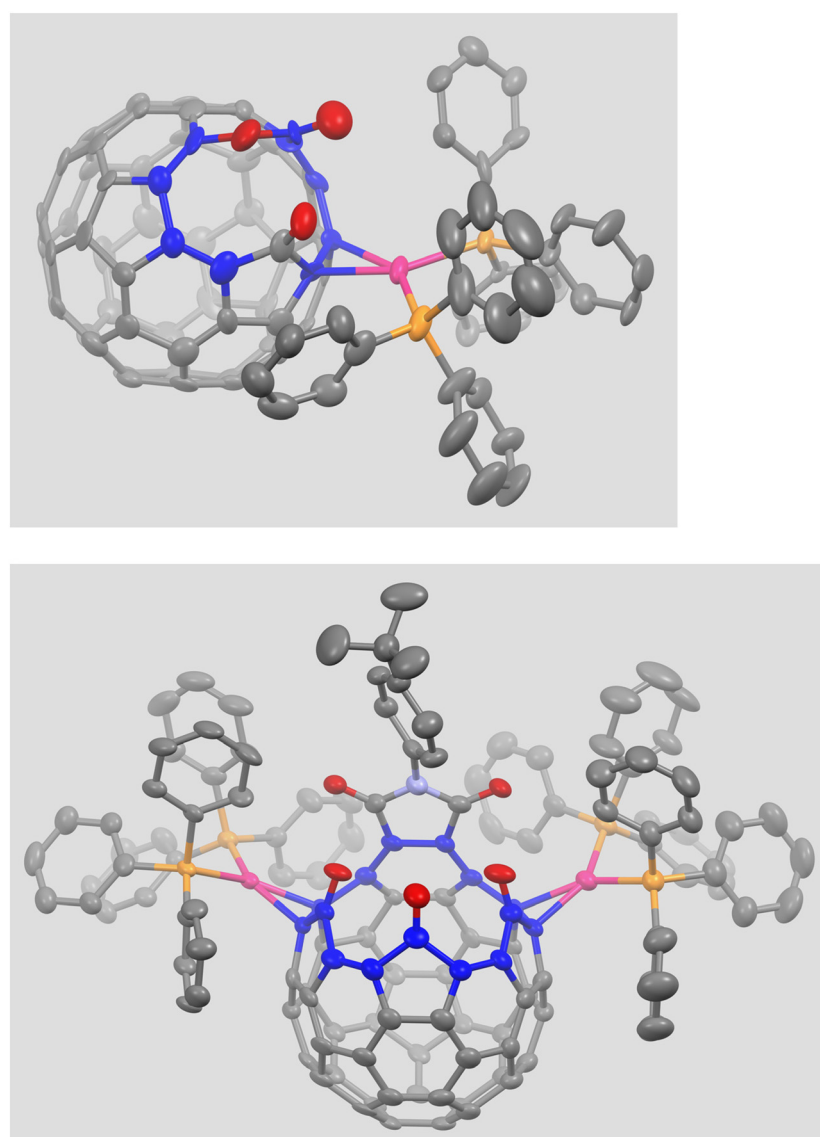


Fig. 6 Top, the structure of the palladium complex ZZYSJG-4. Bottom, the structure of ZZYSJG-5a. Hydrogen atoms were omitted for clarity. Color scheme: carbon, grey except for those on the rim of the opening which are dark blue; oxygen, red; palladium, pink; phosphorus, orange. From data in H. Zhang, Z. Zhou, L. Yang, J. Su, P. Jin and L. Gan, *Organometallics*, 2019, **38**, 3139–43.

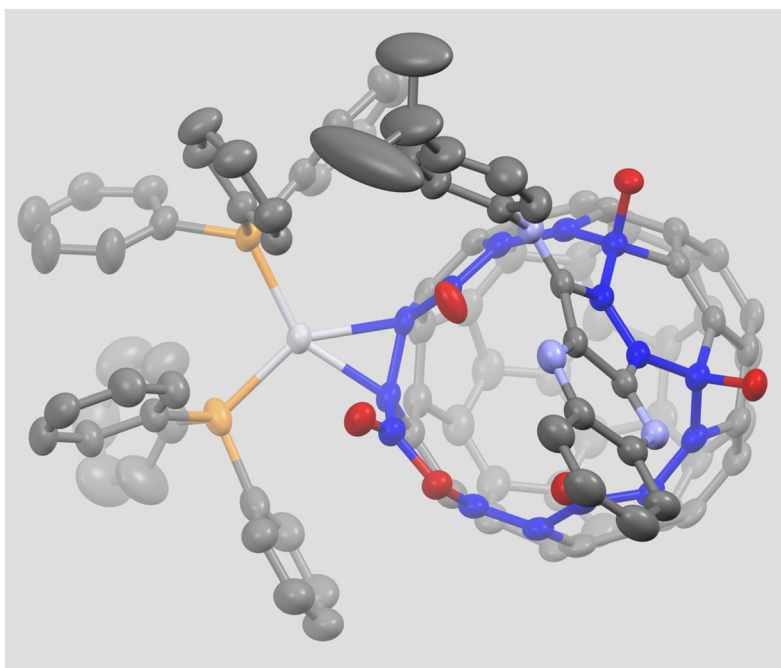


Fig. 7 The structure of the platinum complex **LGG- η^2 -[OCF-2]Pt(PPh₃)₂** with hydrogen atoms and the water molecule inside the cavity removed for clarity. Color scheme: carbon, grey except for those on the rim of the opening which are dark blue; nitrogen, pale blue; oxygen, red; platinum, white; phosphorus, orange. From data in Z. Liu, R. Gao, L. Gan, Synthesis of η^2 -platinum complexes on the rim of open-cage fullerene. *J. Organomet. Chem.*, 2023, **1001**, 122880.

structures have been examined through computational studies.^{40,41}

Conventional η^2 -bonding of (Ph₃P)₂Pt and (Ph₃P)₂Pd units to the rims of open-cage fullerenes

Several open-cage fullerenes have been found to form adducts with (Ph₃P)₂Pt and (Ph₃P)₂Pd units. Fig. 6 shows the structures of two adducts involving coordination of (Ph₃P)₂Pd groups to two different open-cage fullerenes.⁴² In **ZZYSJG-4**, a single (Ph₃P)₂Pd group has bonded to a C-C double bond on the rim of the 11-membered orifice of the cage.⁴² Otherwise, the open cage is unaltered. In **ZZYSJG-5a**, two (Ph₃P)₂Pd groups have been added to C-C double bonds on the rim of a 13-membered ring of different open-cage fullerenes, again without any other alteration of the open cage.⁴² **ZZYSJG-4** and **ZZYSJG-5a** are remarkably stable in solution. Their synthesis from either (Ph₃P)₄Pd or Pd(O₂CCH₃)₂ and Ph₃P was conducted under ambient conditions and the complexes survived chromatographic purification.

The reaction of (Ph₃P)₄Pt with an open-cage fullerene bearing a 19-membered orifice, followed by the reaction of the resulting Pt(PPh₃)₂ adduct with 1,2-diaminobenzene produced **LGG- η^2 -[OCF-2]Pt(PPh₃)₂**, whose structure is shown in Fig. 7.⁴³

Interestingly, a water molecule was drawn into the interior void of the open cage during the synthesis of this molecule. As was true for the palladium complexes described above, **LGG- η^2 -[OCF-2]Pt(PPh₃)₂** was prepared under ambient conditions and is stable to air and chromatography. The platinum atom is η^2 -coordinated to a double bond on the rim of the open-cage fullerene. The C-C bond distance at the coordination site is 1.530(8) Å.

Gan and co-workers have prepared an open-cage fullerene with a 17-membered orifice that has three keto groups, a carboxylate and one ester carbonyl group protruding from the orifice and available for metal binding.⁴⁴ This open-cage fullerene reacts with Rh₂(CO)₄Cl₂ to form several rhodium complexes that have not been obtained in a crystalline form and with (Ph₃P)₄Pt to form **GLLSG-3**, whose structure is shown in Fig. 8. The structure of **GLLSG-3** involves both η^2 -bonding of a (Ph₃P)₂Pt unit to two carbon atoms on the rim of the cage opening and the coordination of a sodium ion to oxygen atoms that are arrayed along the cage opening. Additionally, a water molecule is enclosed within this open-cage fullerene. The top of Fig. 8 shows the asymmetric unit with the sodium ion coordinated by two of the keto groups on the orifice as well as by the carboxylate. The bottom of Fig. 8 shows the dimeric structure, which is formed by packing of two of the open cages about a crystallographic center of symmetry. Each sodium ion acts as a bridge between the two cages and is coordinated by three oxygen

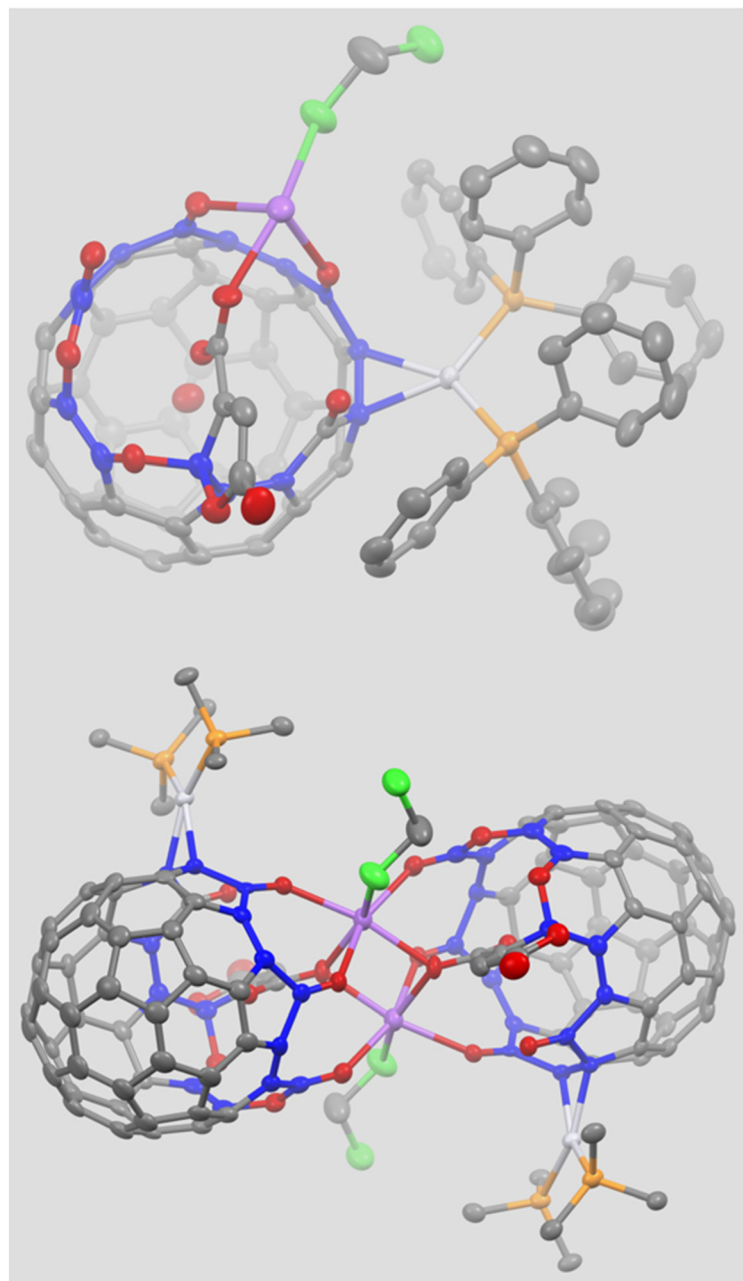


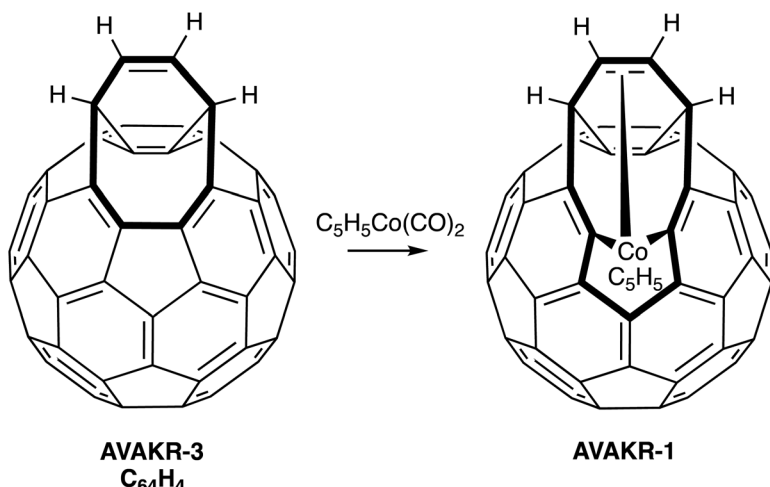
Fig. 8 The structure of GLLSG-3 with hydrogen atoms removed for clarity. Top, the asymmetric unit. Bottom, the centrosymmetric dimer with only the *ipso* carbon atoms of the triphenylphosphine ligands are shown and the interior water molecule removed for clarity. Color scheme: carbon, grey except for those on the rim of the opening which are dark blue; oxygen, red; platinum white; phosphorus, orange; chlorine, green. From data in R. Gao, Z. Liu, Z. Liu, J. Su and L. Gan, *J. Am. Chem. Soc.*, 2023, **145**, 18022–8.

atoms from one cage and by two oxygen atoms from the adjacent cage.

Metal atom coordination and orifice expansion with the bisfulleroid $C_{64}H_4$

Rubin and coworkers prepared the bisfulleroid $C_{64}H_4$ (**AVAKR-3**, see Scheme 5), which contains an eight-mem-

bered opening into the fullerene cage.⁴⁵ The reaction of **AVAKR-3** with $(\eta^5-C_5H_5)Co(CO)_2$ resulted in insertion of the cobalt atom into a C–C bond of the bisfulleroid to produce **AVAKR-1**, as shown in Scheme 5. The structure of **AVAKR-1** is shown in Fig. 9. The cobalt atom is bonded to two carbon atoms of the cage in an η^1 -fashion and to the olefinic bond of the added C_4H_4 unit in an η^2 fashion. The separation between the two carbon atoms of the cage that are connected to cobalt is 2.41(1) Å. The C–Co bond lengths to these cage carbon



Scheme 5 Addition of $(\eta^5\text{-C}_5\text{H}_5)\text{Co}(\text{CO})_2$ to the bisfulleroid, $C_{64}\text{H}_4$.

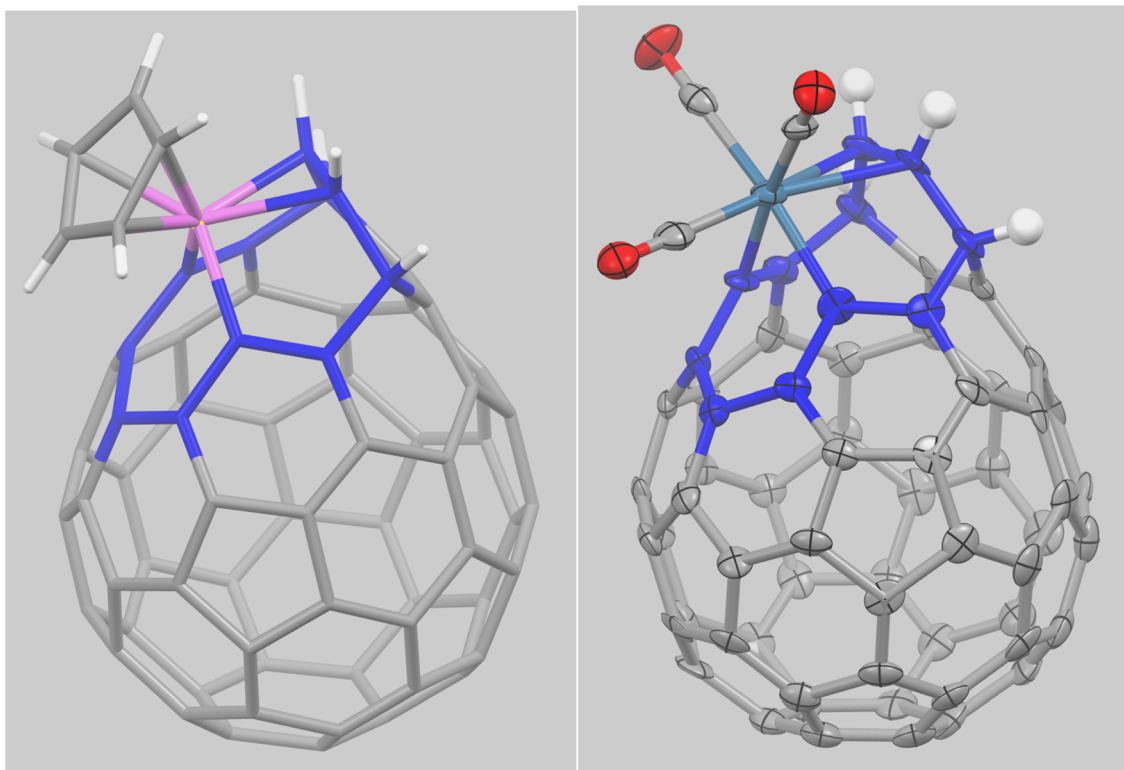


Fig. 9 Left, the structure of AVAKR-1. Color scheme: carbon, grey except for those on the rim of the opening which are dark blue; cobalt, pink, hydrogen, white. From data in M.-J. Arce, A. L. Viado, Y.-Z. An, S. I. Khan, Y. Rubin, *J. Am. Chem. Soc.*, 1996, **118**, 3775–6. Right, the structure of LY-3. Color scheme: carbon, grey except for those on the rim of the opening which are dark blue; osmium, teal, hydrogen, white. From data in S.-T. Lien and W.-Y. Yeh, *J. Organomet. Chem.*, 2012, **715**, 69–72.

atoms are 1.902(8) and 1.923(8) Å. Unfortunately, the reaction conditions used to make AVAKR-1 were not reported. For comparison, $(\eta^5\text{-C}_5\text{H}_5)\text{Co}(\text{CO})_2$ reacts with C_{60} to form the remarkably stable $(\eta^5\text{-C}_5\text{H}_5)\text{Co}(\text{CO})(\eta^2\text{-C}_{60})$, in which the double bond

of the fullerene at a 6:6 ring junction replaces one of the carbonyl ligands on cobalt.⁴⁶

The reaction of AVAKR-3 with $\text{Os}_3(\text{CO})_{10}(\text{NCMe})_2$ in refluxing chlorobenzene solution produces LY-3, whose structure is

shown in Fig. 9.⁴⁷ As with the reaction with $(\eta^5\text{-C}_5\text{H}_5)\text{Co}(\text{CO})_2$, a metal atom is inserted into a carbon–carbon bond of the bisfulleroid. In **LY-3**, the osmium atom is coordinated to the open-cage fullerene through two σ Os–C bonds to carbon atoms formerly part of a pentagonal ring and π coordination to the double bond in the added C_2H_4 unit. The coordination of the osmium atom is completed by three terminal carbon monoxide ligands. For comparison, the reaction of $\text{Os}_3(\text{CO})_{10}(\text{NCMe})_2$ with pristine C_{60} yields $\text{Os}_3(\text{CO})_{10}(\text{NCCH}_3)(\eta^2\text{-C}_{60})$.⁴⁸

Further reactions of **MMK-9**: changes in orifice size caused by reactions of $\text{Ru}_3(\text{CO})_{12}$ with two open-cage fullerene isomers

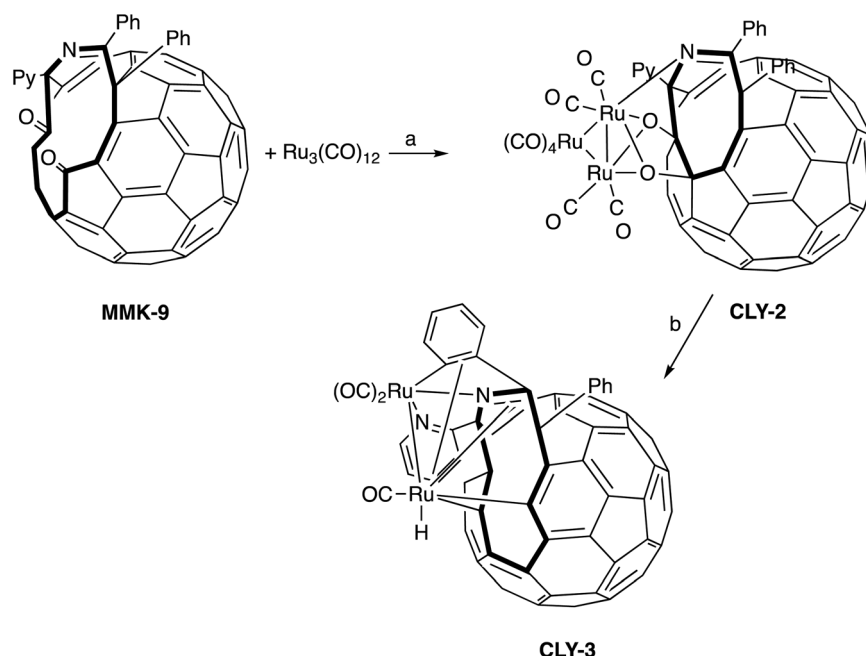
The open-cage fullerene **MMK-9** has a 12-membered ring opening as shown in Fig. 2 and Scheme 6. **MMK-9** reacts with $\text{Ru}_3(\text{CO})_{12}$ to produce **CLY-2**, whose structure is shown in Fig. 10.⁴⁹ In the process, the orifice size has been reduced from a 12-membered ring to an 8-membered ring and a new carbon–carbon bond has been formed between the two ketone carbon atoms in **MMK-9**. However, the bond length of this new C–C bond is rather long, 1.675 Å, when compared to a normal C–C single bond distance of 1.54 Å.

In **CLY2**, only two of the three ruthenium atoms from $\text{Ru}_3(\text{CO})_{12}$ interact with the open-cage fullerene. One of these two ruthenium atoms is coordinated to the two oxygen atoms

of the open-cage fullerene and to a C–C double bond that is not on the rim of the orifice. The other ruthenium atom is coordinated to the two oxygen atoms of the open-cage fullerene and to the imine nitrogen atom of the cage. In contrast, in $\text{Ru}_3(\text{CO})_9(\mu_3\text{-}\eta^2\text{,}\eta^2\text{,}\eta^2\text{-C}_{60})$, which is the product of the reaction between $\text{Ru}_3(\text{CO})_{12}$ and C_{60} , all three ruthenium atoms are coordinated to three C–C double bonds of the fullerene to produce a much simpler structure as seen at the bottom of Fig. 10.⁵⁰

Pyrolysis of **CLY2** under vacuum produces **CLY3** as shown in Scheme 6. In the process, the eight-membered opening in **CLY2** is expanded to a ten-membered opening in **CLY3**, and an $\text{Ru}(\text{CO})_4$ unit is lost. The structure of **CLY3** is shown in Fig. 11. The bonding of the ruthenium atoms to this open-cage fullerene is complicated. One ruthenium atom is connected to two carbon atoms on opposite sides of the orifice, to the C–N double bond, and in an η^2 fashion to two carbon atoms of one of the phenyl rings attached to the cage, while the other ruthenium atom is bonded to the imine nitrogen atom, to the pyridyl nitrogen atom, and to one of the phenyl groups of the cage in an η^1 fashion.

The reaction of **CLY-1b**, which is an isomer of **MMK-9**, with $\text{Ru}_3(\text{CO})_{12}$ followed a different route, one that involves ring expansion rather than ring contraction as shown in Scheme 7. The product of this reaction was **CLY-4** with a 15-membered ring opening, whose structure is shown in Fig. 12. In this product, a single ruthenium atom is connected to the cage through two carbon atoms on either side of the orifice and through an oxygen atom of one of the keto groups.



Scheme 6 Products of the reactions of the open-cage fullerene **MMK-9** with $\text{Ru}_3(\text{CO})_{12}$. Conditions: a, boiling in chlorobenzene for 30 min; b, pyrolysis under vacuum for 30 min.

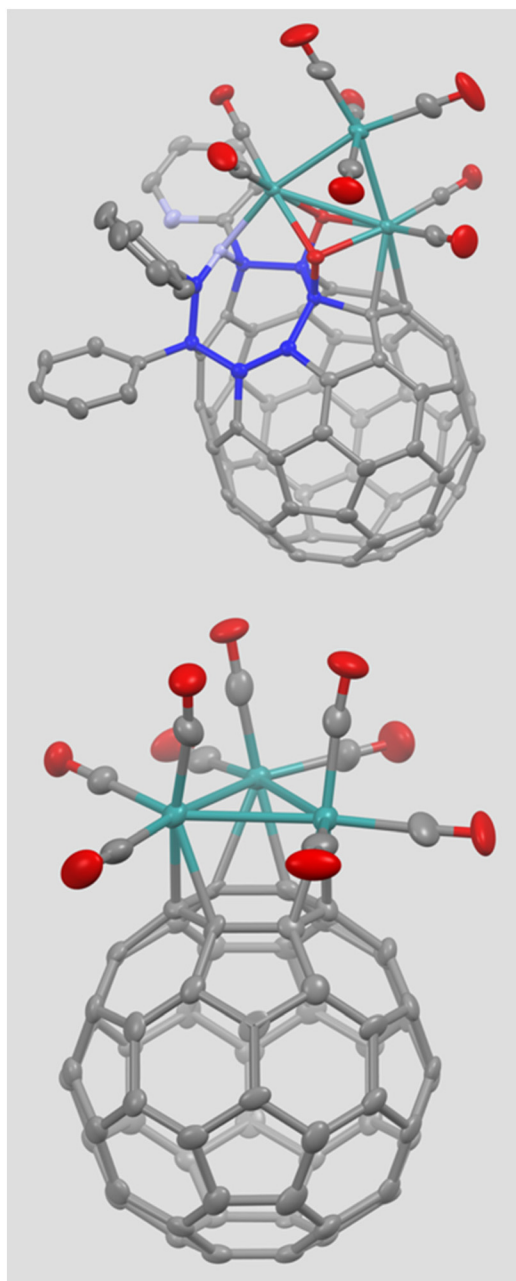


Fig. 10 Top, the structure of the ruthenium complex CLY-2 with hydrogen atoms removed for clarity. Color scheme: carbon, grey except for those on the rim of the opening which are dark blue; oxygen, red; ruthenium, green. From data in C.-S. Chen, Y.-F. Lin and W.-Y. Yeh, *Chem. Eur. J.*, 2014, **20**, 936–40. Bottom: the structure of $\text{Ru}_3(\text{CO})_9(\mu_3-\eta^2, \eta^2, \eta^2-\text{C}_{60})$ from data in H.-F. Hsu and J. R. Shapley, *J. Am. Chem. Soc.*, 1996, **118**, 9192–3.

A novel complex that contains two open-cage fullerenes coordinated to a single nickel(II) ion

As shown in Scheme 8, the open-cage fullerene **ZXG-9** reacts with $\text{NiCl}_2 \cdot n\text{H}_2\text{O}$ in the presence of sodium carbonate to form

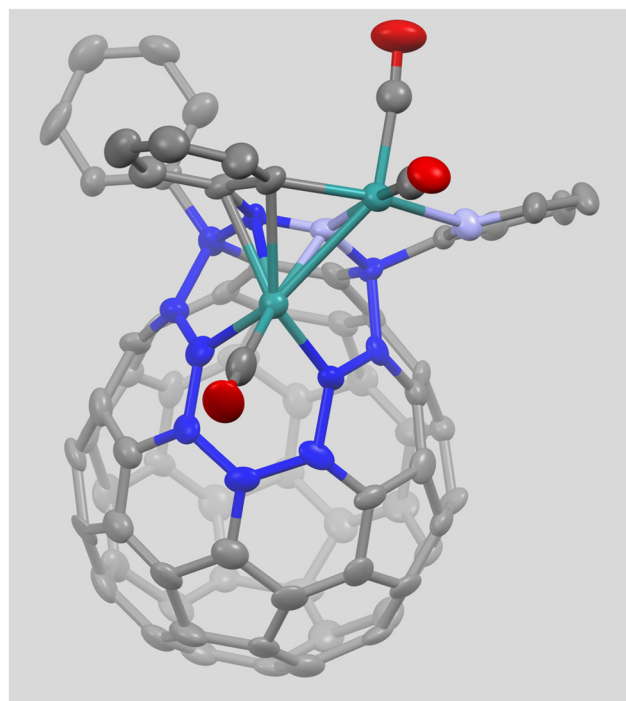
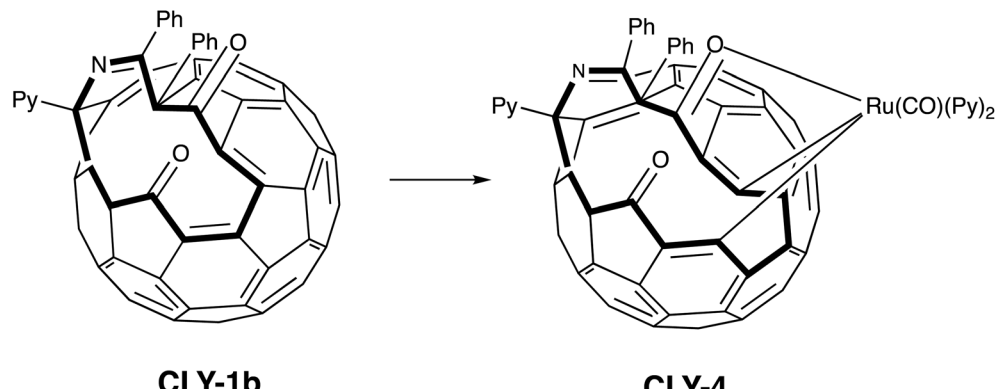


Fig. 11 The structure of the ruthenium complex CLY-3 with hydrogen atoms removed for clarity. Color scheme: carbon, grey except for those on the rim of the opening which are dark blue; oxygen, red; ruthenium, green. From data in C.-S. Chen, Y.-F. Lin and W.-Y. Yeh, *Chem. Eur. J.*, 2014, **20**, 936–40.

the six-coordinate complex **ZXG-10**.⁵¹ This process involves the cleavage of a C–N bond in **ZXG-9** to form a primary amine that coordinates the nickel ion. The nickel ion is bonded to two oxygen atoms and an amine nitrogen from each fullerene. **ZXG-10** appears to be paramagnetic, since it does not exhibit an informative ^1H or ^{13}C spectrum and six-coordinate $\text{Ni}(\text{II})$ complexes are generally paramagnetic. It would be interesting to examine the electrochemical properties of this novel molecule in which two open cages are linked through a nickel ion.

Utilization of the interior space of open-cage fullerenes in bonding alkali metal halides

Gan and coworkers have prepared an open-cage fullerene with a 19-membered orifice that is able to allow halide ions to enter the cavity.⁵² Fig. 14 shows drawings of the product of halide insertion, $\text{SLCGYQSG-Na}_2[\text{Br}@7]_2 \cdot (\text{CH}_3\text{OH})_4$. In the crystal, the complex is a centrosymmetric dimer. The asymmetric unit is shown at the top of this figure. Within this unit, a bromide ion resides at the center of the open cage, while a sodium ion is coordinated to three oxygen atoms from the cage and to two methanol molecules. Dimerization allows each sodium ion to bond with two additional oxygen atoms from keto groups on



Scheme 7 Products of the reactions of the open-cage fullerene **CLY-1b** with $\text{Ru}_3(\text{CO})_{12}$. Conditions: boiling in chlorobenzene, followed by treatment with pyridine.

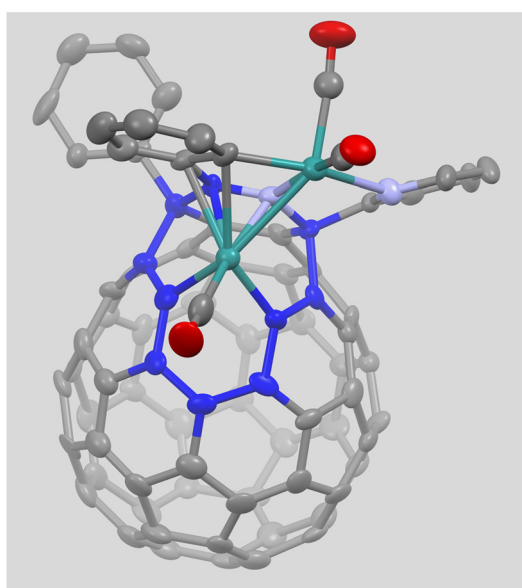
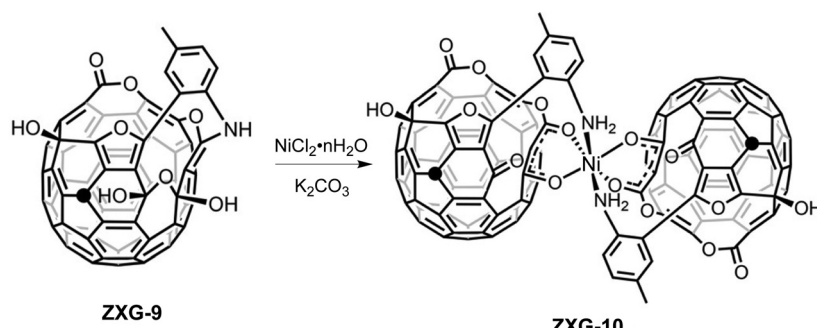


Fig. 12 The structure of the ruthenium complex **CLY-4** with hydrogen atoms removed for clarity. Color scheme: carbon, grey except for those on the rim of the opening which are dark blue; oxygen, red; ruthenium, green. From data in C.-S. Chen, Y.-F. Lin and W.-Y. Yeh, *Chem. Eur. J.*, 2014, **20**, 936–40.

the adjacent open cage, so that each sodium ion is coordinated by a total of seven oxygen atoms. In addition to the bromide ion, fluoride, chloride or iodide ions could be introduced to the interior of this empty-cage fullerene. Encapsulation of each ion was achieved through treatment of the open-cage fullerene in *o*-dichlorobenzene solution with a mixture of hydrohalic acid and acetic acid at temperatures between 60 and 90 °C. The interior of an open-cage fullerene is electron deficient, which provides the driving force for halide ion encapsulation.

Gan and co-workers have also designed and synthesized a novel open-cage fullerene, **GLLSSG6**, that has a coordinating OH group pointing toward the empty cavity.⁵³ This arrangement was created to facilitate the entry of metal ions into the open-cage fullerene. The reaction of **GLLSSG6** with lithium fluoride in a mixture of 1,1,2,2-tetrachloroethane and ethanol yields crystals of **GLLSSG-LiF@6**. Fig. 15 shows the structure of **GLLSSG-LiF@6**, which is reported to have an LiF group bound within the cavity of this open-cage fullerene. The crystallographic data have been interpreted to indicate that the crystal contains a mixture of 8% of the open-cage fullerene, 34% of the open-cage fullerene with water inside, and 58% of the



Scheme 8 Formation of the six-coordinate Ni(II) complex **ZXG-10** from open-cage **ZXG-9** through C–N bond breaking. The black circles show the positions of *t*-BuOO added on the cages. Adapted from Z. Zhou, N. Xin and L. Gan, *Chem. Eur. J.*, 2018, **24**, 451–7.

open cage with LiF inside. The reported Li–F distance is 1.31 Å, which seems quite short given the sum of the ionic radii for Li⁺ and F[−] is 2.09 Å.⁵⁴ Shorter Li–F distances in the range of 1.77–1.81 Å have been observed in some metallacrown complexes.^{55,56} Oddly, the ⁷Li NMR spectrum of **GLLSSG-LiF@6** showed a single resonance, while the ¹⁹F NMR spectrum displayed three resonances. No Li–F coupling was reported. In contrast, the metallacrown complexes of LiF showed Li–F coupling in their ⁷Li and ¹⁹F NMR spectra.^{55,56} A compound similar to **GLLSSG-LiF@6** with a BeF⁺ unit entrapped within this same open cage has also been reported, but salts containing larger ions, such as NaF, MgF₂, CaF₂, and NaCl, could not enter this open-cage fullerene.⁵³

For comparison, the neutral endohedral Li@C₆₀ has been produced by ion implantation through Li⁺ bombardment into a film of C₆₀.⁵⁷ Oxidation of Li@C₆₀ yields the salt (Li@C₆₀)(SbCl₆), which has been examined by single crystal X-ray diffraction.⁵⁸ The structure of (Li@C₆₀)(SbCl₆) shows that the lithium ion is not centered within the cage, but is located near the wall of the cage.

A number of other cases of binding of alkali metal ions to open-cage fullerenes have been reported, but, unfortunately,

no crystallographic data concerning their structures are available.⁵⁹

Macrocyclic ligands based on fullerene cores

The fullerene cage presents a novel framework for the construction of new macrocyclic ligands. For example, Gan suggested that replacement of five carbon atoms in a pentagon of C₆₀ with five oxygen atoms to form keto groups should produce the macrocyclic compound C₅₅O₅ as shown in Scheme 9.⁶⁰ Li and Gan have expanded on this idea and have proposed the synthesis of a range of other macrocyclic ligands based on C₆₀ cores by the removal of some carbon atoms and replacement of other carbon atoms with nitrogen or oxygen atoms.⁶¹ A few of these ligands are shown in Scheme 9.

Proceeding along the opposite direction, a macrocyclic ligand has been used to construct an open-cage metalloazafulerene.⁶² As monitored by electron microscopy, the lead porphyrin shown in Scheme 10 was subjected to an electron beam

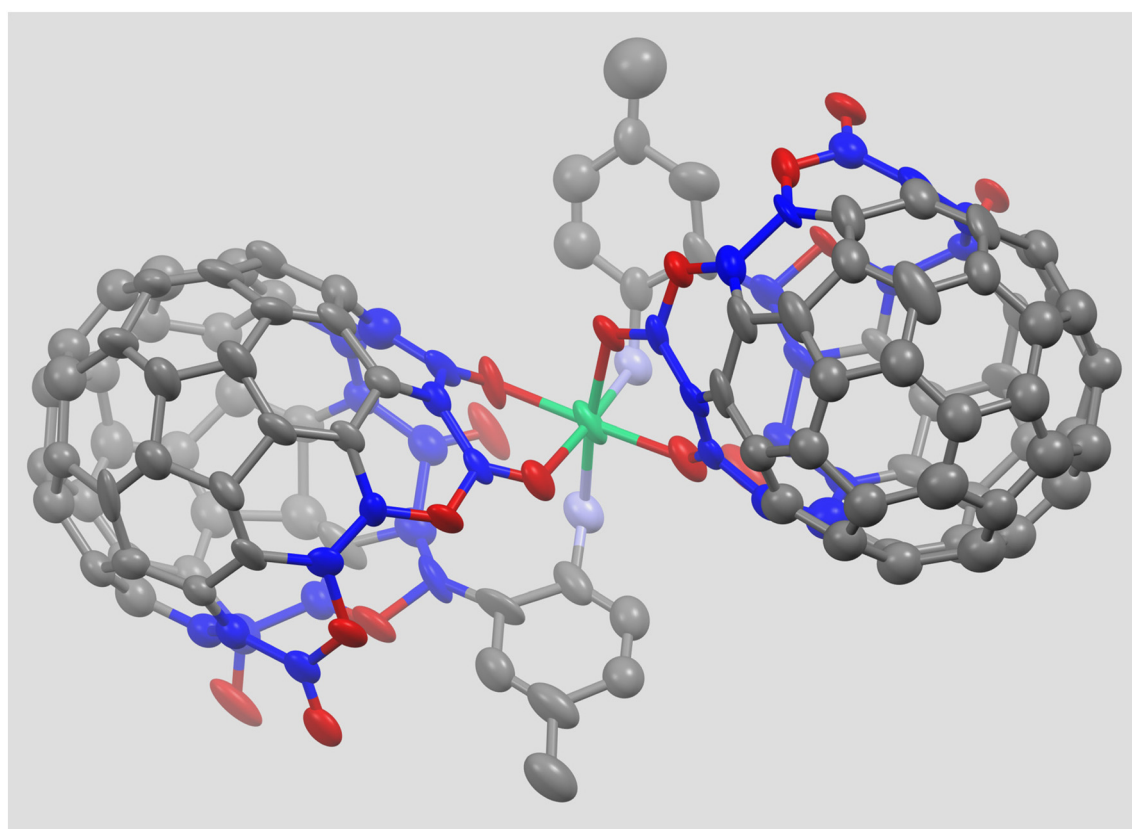


Fig. 13 The structure of **ZXG-10**. Hydrogen atoms, solvate molecules and the two disordered t-butylperoxy groups on the back side of the molecule were omitted for clarity. Color scheme: Ni, green; C, dark grey or deep blue if on the perimeter of the cage opening; O, red; N, light blue. From data in Z. Zhou, N. Xin and L. Gan, *Chem. Eur. J.*, 2018, **24**, 451–7.

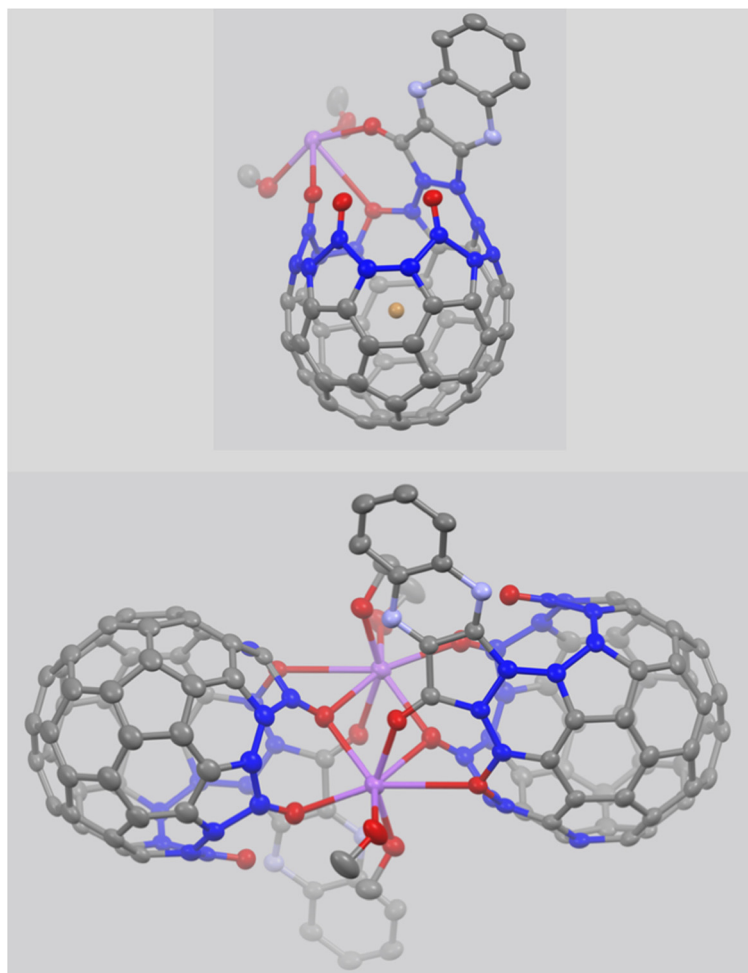


Fig. 14 The structure of SLCGYQSG- $\text{Na}_2[\text{Br}@\mathbf{7}]_2\text{-}(\text{CH}_3\text{OH})_4$. Top, the asymmetric unit. Bottom, the centrosymmetric dimer with the interior bromide ion removed for clarity. Color scheme: Na, pink; C, dark grey or deep blue if on the perimeter of the cage opening; O, red; N, light blue; Br, brown. From data in S. Sun, Z. Liu, F. Colombo, R. Gao, Y. Yu, Y. Qiu, J. Su and L. B. Gan, *Angew. Chem. Int. Ed.*, 2022, **61**, e20221209.

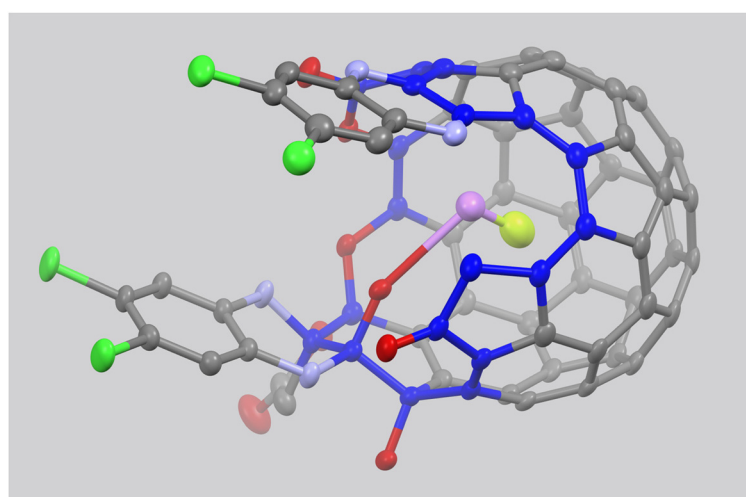
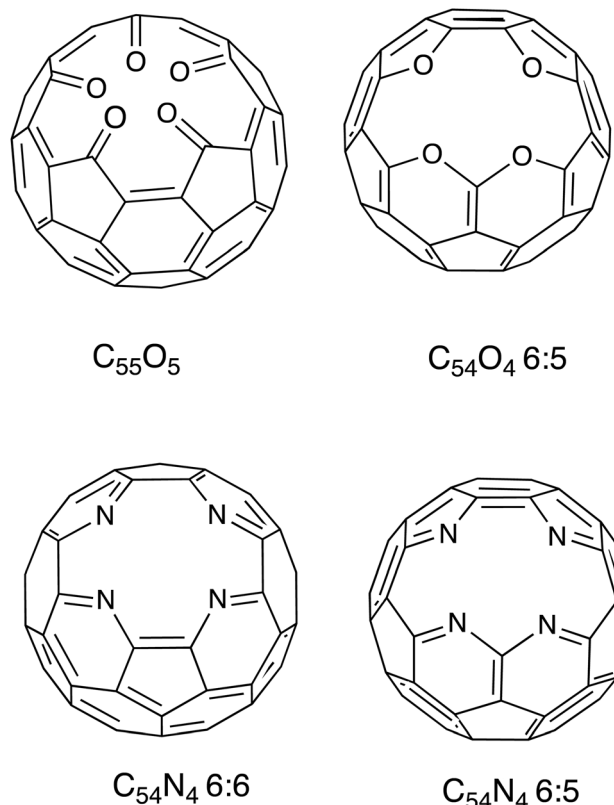


Fig. 15 The structure of GLLLSG-LiF@6. Hydrogen atoms and solvate molecules were omitted for clarity. Color scheme: Li, violet; F, yellow; C, dark grey or deep blue if on the perimeter of the cage opening; O, red; N, light blue; Cl, green. From data in R. Gao, Z. Liu, Z. Liu, T. Liang, J. Su, L. Gan, *Angew. Chem. Int. Ed.*, 2023, **62**, e202300151.



Scheme 9 Potential macrocyclic ligands obtained from C₆₀ by selective replacement or removal of fullerene carbon atoms with nitrogen or oxygen atoms.

that caused the formation of 24 new carbon–carbon bonds and the creation of a new bowl-shaped molecule. It will be interesting to see if more traditional chemical or thermal methods can be used to make macroscopic amounts of this open-cage metalloazafullerene.

Conclusions

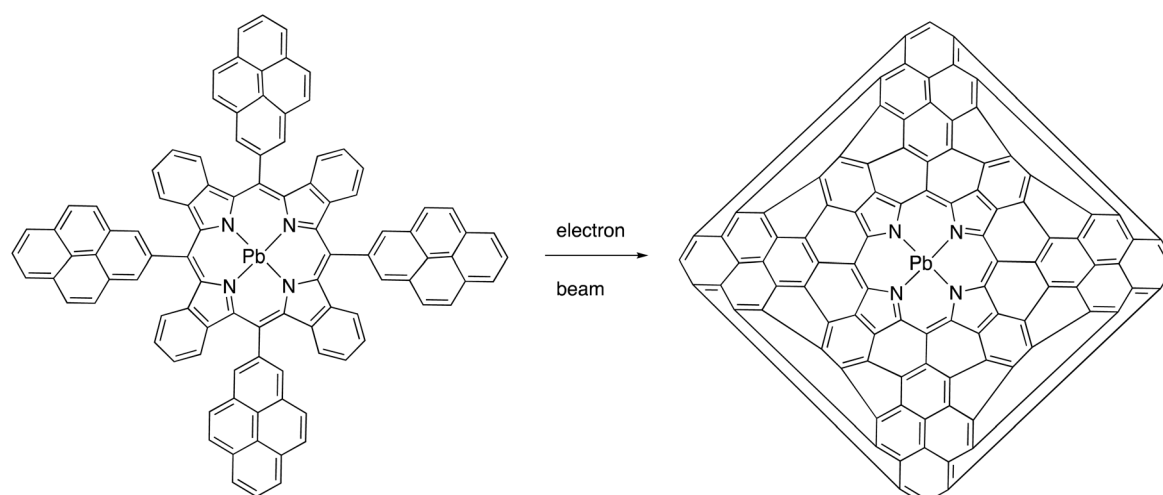
Open-cage fullerenes have been demonstrated to be complex, chemically reactive ligands. From the results described above, a few generalizations can be made.

Reactions of open-cage fullerenes with metal complexes frequently result in bond breaking within the open-cage fullerene. In many cases, such reactions lead to expansion of the orifice size through carbon–carbon bond breaking as shown in Schemes 2, 5, 6 (reaction b), and Scheme 7. In contrast, reaction a in Scheme 6 results in a reduction of the orifice size due to the formation of a new carbon–carbon bond. The reaction in Scheme 8 also involves bond breaking within the open-cage fullerene, but in this case a carbon–nitrogen bond is cleaved.

The rim carbon atoms of open-cage fullerenes are particularly susceptible to addition of (Ph₃P)₂M (M = Pd, Pt) units. Fig. 6–8 show examples. In these addition reactions, the open-cage fullerene undergoes only minor structural changes to accommodate the η^2 -coordination of the metal to one of the double bonds of the rim. Unlike (Ph₃P)₂Pt(η^2 -C₆₀), these (Ph₃P)₂M adducts are remarkably stable to air and chromatography. In a different manner, a (Ph₃P)₂Pt unit has been inserted into a carbon–carbon bond on the rim of an open-cage fullerene as shown in Scheme 2 and Fig. 5.

Anionic forms of open-cage fullerenes frequently form dimers in which pairs of Ag⁺ or Na⁺ ions connect the two cages through coordination to oxygen atoms on the cage surface. Relevant examples include {MMK-9-(OCH₃)₅Ag(AgO₂CCF₃)₂}₂ as shown in Fig. 3, the polymer [{MMK-9-(OCH₃)₅Ag(AgOCH₃)₂·H₂O]_n as shown in Fig. 4, GLLSG-3 as displayed in Fig. 8, and SLCGYQSG-Na₂[Br@7]₂·(CH₃OH)₄ as shown in Fig. 14. The nickel complex ZXG-10 can be viewed similarly with a single Ni²⁺ ion connecting the two anionic open-cage fullerenes as shown in Fig. 13.

Much remains to be learned about the interactions of open-cage fullerenes with metal complexes. Can metal ions larger



Scheme 10 Electron beam synthesis of an open-cage metalloazafullerene.

than Li^+ be encouraged to enter the interior of these open cages? How will redox processes alter the structures of metal complexes of open-cage fullerenes? Will oxidation lead to the ejection of encapsulated anions? Will reduction of the cage encourage the movement of metal ions into the interior void? The research reported here all involves open-cage fullerenes prepared from C_{60} , but open-cage fullerenes can also be made from larger cages such as C_{70} and C_{84} . Will these larger cages provide a more spacious interior void to host various guests?

Conflicts of interest

There are no conflicts to declare.

Acknowledgements

The author thanks his students Dr Amineh Aghabali, Steven Gralinski and Lilia Baldauf for their clever work on open-cage fullerenes and the National Science Foundation [Grant CHE-1807637] for the support.

References

- W. Krätschmer, L. D. Lamb, K. Fostiropoulos and D. R. Huffman, Solid C_{60} : a new form of carbon, *Nature*, 1990, **347**, 354–358.
- A. Hirsch and M. Brettreich, *Fullerenes: Chemistry and Reactions*, Wiley-VCH, Weinheim, Germany, 2005.
- J. C. Hummelen, M. Prato and F. Wudl, There is a Hole in My Bucky, *J. Am. Chem. Soc.*, 1995, **117**, 7003–7004.
- Y. Rubin, Organic approaches to endohedral metallofullerenes: Cracking open or zipping up carbon shells?, *Chem. – Eur. J.*, 1997, **3**, 1009–1016.
- G. C. Vougioukalakis, M. M. Roubelakis and M. Orfanopoulos, Open-cage fullerenes: towards the construction of nanosized molecular containers, *Chem. Soc. Rev.*, 2010, **39**, 817–844.
- L. Gan, Molecular Containers Derived from [60]Fullerene through Peroxide Chemistry, *Acc. Chem. Res.*, 2019, **52**, 1793–1801.
- S. Bloodworth and R. J. Whitby, Synthesis of endohedral fullerenes by molecular surgery, *Commun. Chem.*, 2022, **5**, 121.
- K. Komatsu, M. Murata and Y. Murata, Encapsulation of molecular hydrogen in fullerene C_{60} by organic synthesis, *Science*, 2005, **307**, 238–240.
- K. Kurotobi and Y. Murata, A single molecule of water encapsulated in fullerene C_{60} , *Science*, 2011, **333**, 613–616.
- Y. Murata, M. Murata and K. Komatsu, Synthesis, Structure, and Properties of Novel Open-Cage Fullerenes Having Heteroatom(s) on the Rim of the Orifice, *Chem. – Eur. J.*, 2003, **9**, 1600–1609.
- A. Rodriguez-Forte, A. L. Balch and J. M. Poblet, Endohedral metallofullerenes: a unique host-guest association, *Chem. Soc. Rev.*, 2011, **40**, 3551–3563.
- A. A. Popov, S. Yang and L. Dunsch, Endohedral Fullerenes, *Chem. Rev.*, 2013, **113**, 5989–6113.
- M. Yamada, T. Akasaka and S. Nagase, Endohedral Metal Atoms in Pristine and Functionalized Fullerene Cages, *Acc. Chem. Res.*, 2010, 92–102.
- T. Li and H. C. Dorn, Biomedical Applications of Metal-Encapsulated Fullerene Nanoparticles, *Small*, 2017, **13**, 1603152.
- R. D. Bolkskar, A. Borel, G. González, L. Helm, A. E. Merbach, B. Sitharaman and L. J. Wilson, Water-Soluble Gadofullerenes: Toward High-Relaxivity, pH-Responsive MRI Contrast Agents, *J. Am. Chem. Soc.*, 2010, **132**(14), 4980–4981.
- K. B. Ghiassi, M. M. Olmstead and A. L. Balch, Gadolinium-containing endohedral fullerenes: structures and function as magnetic resonance imaging (MRI) agents, *Dalton Trans.*, 2014, **43**, 7346–7358.
- E. Ieazzi, J. Duchamp, K. Fletcher, T. Glass and H. Dorn, Lutetium-based Trimetallic Nitride Endohedral Metallofullerenes: New Contrast Agents, *Nano Lett.*, 2002, **2**, 1187–1190.
- M. D. Shultz, J. C. Duchamp, J. D. Wilson, C.-Y. Shu, J. Ge, J. Zhang, H. W. Gibson, H. L. Fillmore, J. I. Hirsch, H. C. Dorn and P. P. Fatouros, Encapsulation of a Radiolabeled Cluster Inside a Fullerene Cage, $^{177}\text{Lu}_x\text{Lu}_{(3-x)}\text{N}@\text{C}_{80}$: An Interleukin-13-Conjugated Radiolabeled Metallofullerene Platform, *J. Am. Chem. Soc.*, 2010, **132**, 4980–4981.
- K. Watanabe, M. Komatsu, Y. Niidome, M. Murata, Y. Murata, K. Komatsu and N. Nakashima, Electrochemistry of an Open-Cage Fullerene Embedded in a Film of Hydrophobic Ammonium Ion on an Electrode, *J. Phys. Chem. C*, 2007, **111**, 6500–6504.
- L. Balch and K. Winkler, Two-Component Polymeric Materials of Fullerenes and the Transition Metal Complexes: A Bridge Between Metal-Organic Frameworks and Conducting Polymers, *Chem. Rev.*, 2016, **116**, 3812–3882.
- L. Balch and K. Winkler, Electrochemistry of fullerene/transition metal complexes: Three decades of progress, *Coord. Chem. Rev.*, 2021, **438**, 213623.
- P. J. Fagan, J. C. Calabrese and B. Malone, The Chemical Nature of Buckminsterfullerene (C_{60}) and the Characterization of a Platinum Derivative, *Science*, 1991, **252**, 1160–1161.
- L. Balch, V. J. Catalano, J. W. Lee, M. M. Olmstead and S. R. Parkin, $(\eta^2\text{C}_{70})\text{Ir}(\text{CO})\text{Cl}(\text{PPh}_3)_2$. The Synthesis and Structure of an Organometallic Derivative of a Higher Fullerene, *J. Am. Chem. Soc.*, 1991, **113**, 8953–8954.
- L. Balch and M. M. Olmstead, Reactions of Transition Metal Complexes with Fullerenes (C_{60} , C_{70} , etc.) and Related Materials, *Chem. Rev.*, 1998, **98**, 2123–2165.

25 D. V. Konarev and R. N. Lyubovskaya, New approaches to the synthesis of transition-metal complexes of fullerenes C_{60} and C_{70} , *Russ. Chem. Rev.*, 2016, **85**, 1215–1228.

26 F. L. Bowles, M. M. Olmstead and A. L. Balch, Preparation and Crystallographic Characterization of $C_{60}\{\eta^1\text{-Ru}(\text{CO})_2(\eta^5\text{-C}_5\text{H}_5)\}_2$: A Locally Crowded Organometallic Fullerene Without the Usual η^2 -Bonding, *J. Am. Chem. Soc.*, 2014, **136**, 3338–3341.

27 K. Lee, H. Song and J. T. Park, [60]Fullerene-Metal Cluster Complexes: Novel Bonding Modes and Electronic Communication, *Acc. Chem. Res.*, 2003, **36**, 78–86.

28 W.-Y. Yeh, Coordination and reactivity of functionalized fullerenes, open-cage fullerenes, and endohedral metallofullerenes by organometallic complexes, *J. Organomet. Chem.*, 2015, **784**, 13–23.

29 M. A. Petrukhina and L. T. Scott, Coordination chemistry of buckybowl: from corannulene to a hemifullerene, *Dalton Trans.*, 2005, 2969–2975.

30 Z. Zhou and M. A. Petrukhina, Planar, curved and twisted molecular nanographenes: Reduction-induced alkali metal coordination, *Coord. Chem. Rev.*, 2023, **486**, 215144.

31 S.-C. Chuang, Y. Murata, M. Murata and K. Komatsu, An Orifice-Size Index for Open-Cage Fullerenes, *J. Org. Chem.*, 2007, **72**, 6447–6453.

32 A. Aghabali, S. Jun, M. M. Olmstead and A. L. Balch, Silver (I)-Mediated Modification, Dimerization and Polymerization of an Open-Cage Fullerene, *J. Am. Chem. Soc.*, 2016, **138**, 16459–16465.

33 M. Sawamura, H. Iikura and E. J. Nakamura, The First Pentahaptfullerene Metal Complexes, *J. Am. Chem. Soc.*, 1996, **118**, 12850–12851.

34 M. Sawamura, Y. Kuninobu, M. Togano, Y. Matsuo, M. Yamanaka and E. Nakamura, Hybrid of Ferrocene and Fullerene, *J. Am. Chem. Soc.*, 2002, **124**, 9354–9355.

35 M. M. Olmstead, K. Maitra and A. L. Balch, Formation of a Curved Silver Nitrate Network That Conforms to the Shape of C_{60} and Encapsulates the Fullerene - Structural Characterization of $C_{60}\{\text{Ag}(\text{NO}_3)\}_5$, *Angew. Chem., Int. Ed.*, 1999, **38**, 231–233.

36 H. Schmidbaur and A. Schier, Argentophilic interactions, *Angew. Chem., Int. Ed.*, 2015, **54**, 746–784.

37 S. R. Gralinski, M. Roy, L. M. Baldauf, M. M. Olmstead and A. L. Balch, Introduction of a $(\text{Ph}_3\text{P})_2\text{Pt}$ Group into the Rim of an Open-cage Fullerene by Breaking a Carbon-Carbon Bond, *Chem. Commun.*, 2016, **138**, 16459–16465.

38 L. Edelbach, R. J. Lachicotte and W. D. Jones, Mechanistic Investigation of Catalytic Carbon-Carbon Bond Activation and Formation by Platinum and Palladium Phosphine Complexes, *J. Am. Chem. Soc.*, 1998, **120**, 2843–2853.

39 R. M. Shaltout, R. Sygula, A. Sygula, F. R. Fronczek, G. G. Stanley and P. W. Rabideau, The First Crystallographically Characterized Transition Metal Buckybowl Compound: $C_{30}\text{H}_{12}$ Carbon-Carbon Bond Activation by $\text{Pt}(\text{PPh}_3)_2$, *J. Am. Chem. Soc.*, 1998, **120**, 835–836.

40 J. M. Poblet, K. Winkler, M. Cancilla, A. Hayashi, C. B. Lebrilla and A. L. Balch, Geometric and Electronic Structure of Metal-Cage Fullerenes, $C_{59}\text{M}$ ($\text{M} = \text{Pt, Ir}$) Obtained by Laser Ablation of Electrochemically Deposited Films, *Chem. Commun.*, 1999, 493–494.

41 A. Hayashi, Y. Xie, J. M. Poblet, J. M. Campanera, C. B. Lebrilla and A. L. Balch, Mass Spectrometric and Computational Studies of Heterofullerenes $[(\text{C}_{58}\text{Pt})^-, (\text{C}_{59}\text{Pt})^+]$ Obtained by Laser Ablation of Electrochemically Deposited Films, *J. Phys. Chem. A*, 2004, **108**, 2192–2198.

42 H. Zhang, Z. Zhou, L. Yang, J. Su, P. Jin and L. Gan, Selective Addition of Palladium on the Rim of Open-Cage Fullerenes To Form Mononuclear and Dinuclear Complexes, *Organometallics*, 2019, **38**, 3139–3143.

43 Z. Liu, R. Gao and L. Gan, Synthesis of η^2 -platinum complexes on the rim of open-cage fullerene, *J. Organomet. Chem.*, 2023, **1001**, 122880.

44 R. Gao, Z. Liu, Z. Liu, J. Su and L. Gan, Open-Cage Fullerene as a Macroyclic Ligand for Na, Pt, and Rh Metal Complexes, *J. Am. Chem. Soc.*, 2023, **145**, 18022–18028.

45 M.-J. Arce, A. L. Viado, Y.-Z. An, S. I. Khan and Y. Rubin, Triple Scission of a Six-Membered Ring on the Surface of C_{60} via, Consecutive Pericyclic Reactions and Oxidative Cobalt Insertion, *J. Am. Chem. Soc.*, 1996, **118**, 3775–3776.

46 Y. Hashikawa, M. Murata, A. Wakamiya and Y. Murata, Co (I)-Mediated Removal of Addends on the C_{60} Cage and Formation of the Monovalent Cobalt Complex $\text{CpCo}(\text{CO})(\eta^2\text{-}C_{60})$, *Org. Lett.*, 2016, **18**, 6348–6351.

47 S.-T. Lien and W.-Y. Yeh, Complexation and activation of the bisfulleroid $C_{64}\text{H}_4$ with triosmium carbonyl clusters, *J. Organomet. Chem.*, 2012, **715**, 69–72.

48 J. T. Park, H. Song, J.-J. Cho, M.-K. Chung, J.-H. Lee and I.-H. Suh, Synthesis and Characterization of $\eta^2\text{-}C_{60}$ and $\mu_3\text{-}\eta^2\text{-}\eta^2\text{-}C_{60}$ Triosmium Cluster Complexes, *Organometallics*, 1998, **17**, 227–236.

49 C.-S. Chen, Y.-F. Lin and W.-Y. Yeh, Activation of Open-Cage Fullerenes with Ruthenium Carbonyl, *Chem. – Eur. J.*, 2014, **20**, 936–940.

50 H.-F. Hsu and J. R. Shapley, $\text{Ru}_3(\text{CO})_9(\mu_3\text{-}\eta^2\text{-}\eta^2\text{-}C_{60})$: A Cluster Face-Capping, Arene-Like Complex of C_{60} , *J. Am. Chem. Soc.*, 1996, **118**, 9192–9193.

51 Z. Zhou, N. Xin and L. Gan, Synthesis of Metal Complexes with an Open-Cage Fullerene as the Ligand, *Chem. – Eur. J.*, 2018, **24**, 451–457.

52 S. Sun, Z. Liu, F. Colombo, R. Gao, Y. Yu, Y. Qiu, J. Su and L. B. Gan, Open-Cage Fullerene as Molecular Container for F^- , Cl^- , Br^- and I^- , *Angew. Chem., Int. Ed.*, 2022, **61**, e20221209.

53 R. Gao, Z. Liu, Z. Liu, T. Liang, J. Su and L. Gan, Open-Cage Fullerene as a Selective Molecular Trap for $\text{LiF}/[\text{BeF}]^+$, *Angew. Chem., Int. Ed.*, 2023, **62**, e202300151.

54 E. Housecraft and A. G. Sharpe, *Inorganic Chemistry*, Pearson, New York, 5th edn, 2018, pp. 1158–1159.

55 M.-L. Lehaire, R. Scopelliti, H. Piotrowski and K. Severin, Selective Recognition of Fluoride Anion Using a Li^+ - Metallacrown Complex, *Angew. Chem., Int. Ed.*, 2002, **41**, 1419–1422.

56 M.-L. Lehaire, R. Scopelliti and K. Severin, Stabilization of Molecular LiF and LiFHF inside Metallamacrocyclic Hosts, *Inorg. Chem.*, 2002, **41**, 5466–5474.

57 R. Tellgmann, N. Krawez, S. H. Lin, I. V. Hertel and E. E. B. Campbell, Endohedral fullerene production, *Nature*, 1996, **382**, 407–408.

58 S. Aoyagi, E. Nishibori, H. Sawa, K. Sugimoto, M. Takata, Y. Miyata, R. Kitaura, H. Shinohara, H. Okada, T. Sakai, Y. Ono, K. Kawachi, K. Yokoo, S. Ono, K. Omote, Y. Kasama, S. Ishikawa, T. Komuro and H. Tobita, A layered ionic crystal of polar Li@C₆₀ superatoms, *Nat. Chem.*, 2010, **2**, 678–683.

59 Y. Hashikawa and Y. Murata, Cation recognition on a fullerene-based macrocycle, *Chem. Sci.*, 2020, **11**, 12428–12435.

60 L. B. Gan, Peroxide-Mediated Selective Cleavage of [60] Fullerene Skeleton Bonds: Towards the Synthesis of Open-Cage Fulleroid C₅₅O₅, *Chem. Rec.*, 2015, **15**, 189.

61 Y. Li and L. B. Gan, [60]Fullerene-Based Macrocycle Ligands, *Chem. – Eur. J.*, 2017, **23**, 10485–10490.

62 H. Hoelzel, S. Lee, K. Y. Amsharov, N. Jux, K. Harano, E. Nakamura and D. Lungerich, Time-resolved imaging and analysis of the electron beam-induced formation of an open-cage metallo-azafullerene, *Nat. Chem.*, 2023, **15**, 1444–1451.